UNMANNED AERIAL VEHICLES (UAV) FOR COST EFFECTIVE AERIAL ORTHOPHOTOS AND DIGITAL SURFACE MODELS (DSM)

Mark C. Harvey[1], Sophie Pearson[2], Kenneth B. Alexander[3], Julie Rowland[1] and Phil White[4]

[1]School of Environment, University of Auckland, Auckland, New Zealand

[2]GNS Science, New Zealand

[3]Institute of Earth Science and Engineering, Auckland, New Zealand

[4]Panda Geoscience Limited, Auckland, New Zealand

mhar098@aucklanduni.ac.nz

Keywords: *UAV, DEM, DSM, digital, elevation, model, drone, unmanned, aerial, vehicle, geothermal.*

ABSTRACT

High quality aerial photos (orthophotos) and digital surface models (DSM) are invaluable at all phases of geothermal exploration and development including geological, geochemical and geophysical surveys, environmental baseline studies, geotechnical studies, civil works, steam field design, plant design and construction. High resolution (<0.1m) imagery and data are typically collected by sensors mounted on board manned light aircraft. Lower resolution imagery (>0.5m) can be obtained from satellite imagery. A rapidly improving alternative is the collection of imagery from sensors mounted on unmanned aerial vehicles (UAVs). Such imagery can be used to produce high resolution (<0.1m) orthophotos, or DSM's of comparable quality to LiDAR. UAVs offer orthophotos and DSM's at a fraction of the cost of manned aircraft, at a higher resolution than is currently available from satellite. The economics of UAV's allow for cost effective repeat surveying, useful for progress reporting during construction, or potentially monitoring subsidence due to fluid extraction. In this paper, we describe a case study of a UAV-derived DSM produced from aerial images of the Poihipi geothermal steam field in New Zealand. The DSM is compared to a commercially produced LiDAR DEM from the same area.

1. INTRODUCTION

A digital surface model (DSM) is a virtual representation of the earth's surface and includes all objects on it, such as vegetation and buildings. Digital Elevation Models (DEM) are a representation of the earth's bare surface without vegetation or buildings (Priestnall et al., 2000).

High resolution (<0.1m) DSM and DEM are typically collected by sensors mounted on board manned light aircraft. Lower resolution imagery (>0.5m) can be obtained from satellite (Lejot et al., 2007). Sensors include Light Detection and Ranging (LiDAR), optical cameras (photogrammetry), or infrared.

Photogrammetry is a technology that allows measurements to be made from photographs, and for the reconstruction of three dimensional information (i.e. DSM) from a mosaic of overlapping, two dimensional photographs (Li et al., 2010).

Photogrammetry is well established technology, but recent advances in unmanned aerial vehicles (UAV) equipped with global positioning systems (GPS) and digital cameras are reducing the cost of collecting imagery. Modern desktop and cloud computing power allows for routine post processing of large numbers of individual image photos. The individual photos are combined into aerial orthophotos and DSM/DEM of comparable quality (<0.1m) to airborne LiDAR (Harwin & Lucieer, 2012; Fonstad et al., 2013).

Regulations covering the use of UAVs varies according to jurisdiction, UAV size and purpose (i.e. commercial or recreational). In New Zealand, relevant legislation is described in Civil Aviation Rules Part 101 (NZ CAA, 2014).

High quality aerial photos (orthophotos) and DSM's are useful at all phases of geothermal exploration and development. Examples include maps for geological, geochemical and geophysical surveys (van der Meer et al., 2014), environmental baseline studies, geotechnical studies, civil works, steam field design, plant design and construction (Li et al., 2010).

The economics and speed of this approach allows for cost effective repeat surveying, useful for progress reporting during civil works or construction.

2. METHODS

2.1 Field Methods

Imagery was collected using a modified DJI Phantom 2 Vision+ quadcopter (Figure 1). The quadcopter was modified by the replacement of the stock camera with a Canon A2400 camera (16MP); the stock camera has a wide angle (fish-eye) lens that is not ideal for photogrammetry. The Canon camera was programmed with an intervelometer script in order to autonomously capture images (5 second intervals) during flight.

Figure 1. DJI Phantom Vision 2+ quadcopter

An appropriate flight plan was determined using DJI Ground Station® software. The flight plan was then uploaded to the quadcopter's flight controller using the DJI Vision App. Accordingly, both in-flight navigation and image capture were autonomous.

Ground control points (GCP) were established prior to flight by placing yellow duct tape on established survey bench marks. The benchmark locations were last checked in 2013 and the average elevation (Z) error was 3.8mm. Most benchmarks were located on geothermal steam line footings, immediately adjacent to Poihipi Road, Taupo.

Three flights were conducted, each of approximately 17 minutes duration giving a total flight time of about 50 minutes. Flight altitude was 120m (relative to the launch point), with a ground speed of 4 m/s.

Fight conditions were windy with a maximum wind speed of ~36 km/hr. Although clear with good visibility, the flight was conducted with the sun at a relatively low angle with respect to the horizon (mid-July afternoon in the Southern Hemisphere).

2.2 Image Processing

317 overlapping images were processed using Agisoft Photoscan®, commercial photogrammetry software (Figure 2). Coordinates for 11 GCP were used to georeference the resulting orthophoto (Figure 3a) and DEM (Figure 3b).

Three additional GCP were used to test the accuracy of the orthophoto and DEM, and so were not utilized in the georeferencing process. The ground resolution and position error of the DSM and orthophoto was determined automatically by Photoscan®.

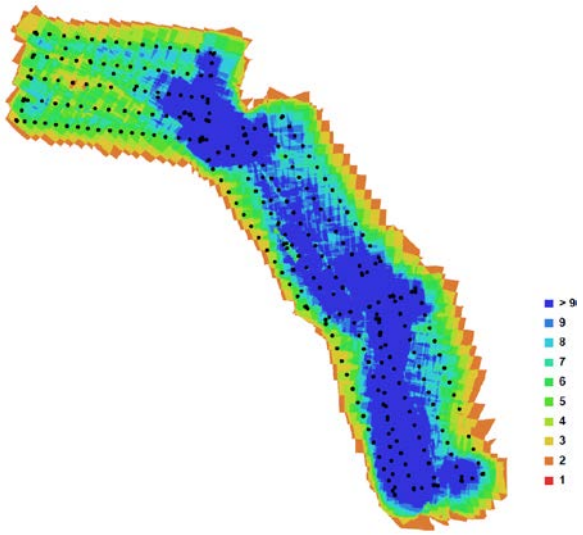

Figure 2: Camera locations and image overlap (numbers refer to number of images that capture that area).

2. RESULTS

Image processing provided and orthophoto (Figure 3a) and DSM (Figure 3b) with 0.61km^2 coverage area. Ground resolution was 3cm (pixel size). Positional error calculated for check points is shown in Table 1.

Table 1. Positional error estimated using GCP

	X Error	Y Error	Z Error	Error
Point	-0.016	0.005	-0.231	0.232
Point	-0.141	0.060	-0.503	0.526
Point	0.096	-0.047	0.022	0.107

4. DISCUSSION

Smaller areas have been expanded to show the quality of the imagery (Figure 4a, 4b, 5a and 5b). The orthophoto and DSM have a ground resolution of 0.03m (pixel size). This is almost two orders of magnitude higher than DEM imagery supplied by Contact Energy Ltd (2m pixel size), from a previous large scale survey of the same area (compare Figure 4b to Figure 4c).

The DSM images (Figure 3b, 4b and 5b) show both the land surface, and buildings/vegetation covering the ground. It is possible to produce DEMs (vegetation and buildings can be removed using tools within Agisoft Photoscan®), but this was not attempted.

Average positional error (0.29m) was calculated from three check points (Table 1). Both ground resolution and positional error are a function of the following factors, i) number of GCP, ii) even distribution of GCP, iii) camera quality, iii) meteorological conditions, and iv) flight altitude. Accordingly, improvements in ground resolution (< 0.03m) and particularly positional error (<0.04m) are achievable and have been reported elsewhere (Harwin & Lucieer, 2012).

5. CONCLUSION

Our study has demonstrated a low cost approach to the production of georeferenced DSM's and orthophotos from aerial images captured by UAV. The ground resolution and position error of our DSM and orthophoto is comparable to commercially produced LiDAR and aerial imagery obtained from manned aircraft.

High quality DSM and orthophotos are useful in all phases of geothermal exploration and development including geological, geochemical and geophysical surveys, environmental baseline studies, geotechnical studies, civil works, steam field design, plant design and construction.

Figure 3a: Orthophoto (UTM WGS84). Yellow square shows detail area in Figures 4(a-c).

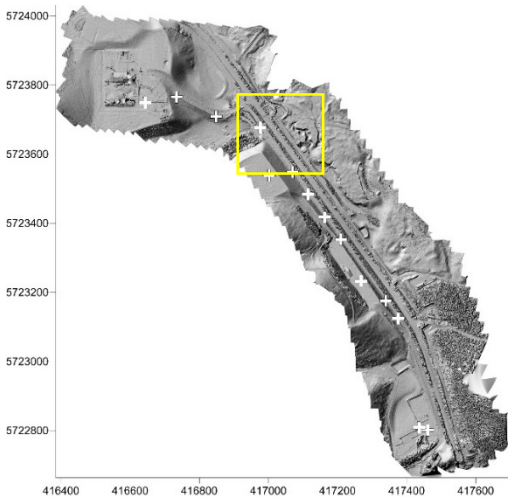

Figure 3b: DSM (UTM WGS84). White crosses are control points.

Figure 4a. Orthophoto cropped area (UTM WGS84). Yellow square shows area of fine detail in Figures 5a & 5b.

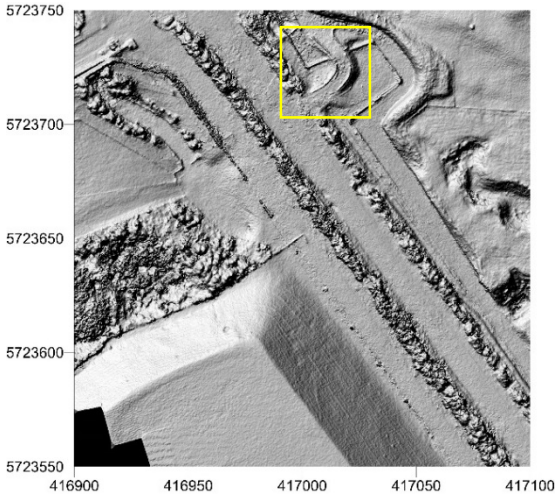

Figure 4b. DSM cropped area (UTM WGS84). Yellow square shows area of fine detail (Figures 5a and 5b).

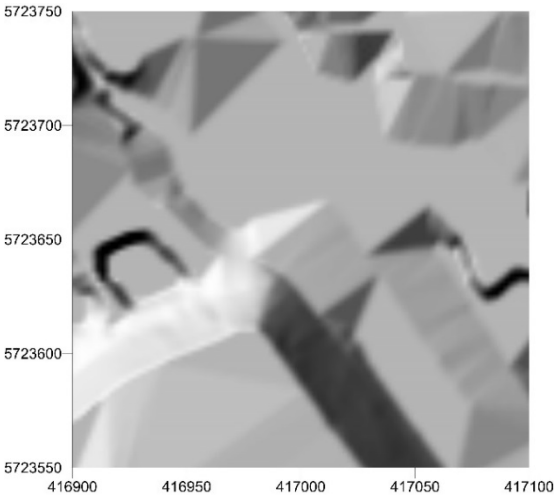

Figure 4c. DEM (2m) cropped area (cf. Figure 4b)(UTM WGS84).

Figure 5a. Orthophoto fine detail (UTM WGS84).

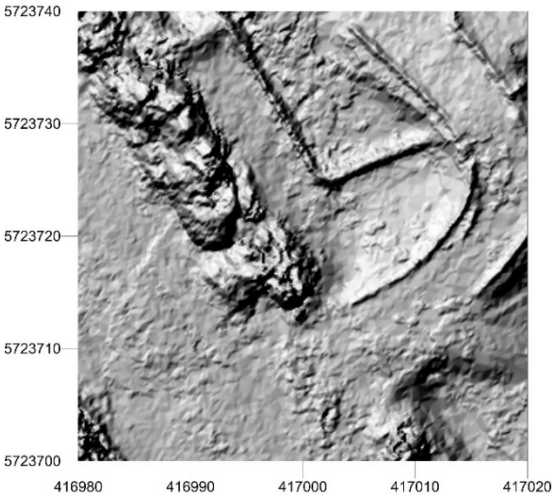

Figure 5b. DSM fine detail (UTM WGS84).

ACKNOWLEDGEMENTS

The authors would like to acknowledge and thank GNS for providing financial support to this project. We would also like to thank Contact Energy Ltd for providing levelling data and access to surveyed areas.

REFERENCES

Axelsson, P. (2000). DEM generation from laser scanner data using adaptive TIN models. Int. Arch. Photogram. Rem. Sens., 33(B4/1; PART 4), 111-118.

New Zealand Civil Aviation Authority (2014), http://www.caa.govt.nz/rpas/

Fonstad, M. A., Dietrich, J. T., Courville, B. C., Jensen, J. L. and Carbonneau, P. E. (2013), Topographic structure from motion: a new development in photogrammetric measurement. Earth Surf. Proc. Land, 38: 421–430. doi: 10.1002/esp.3366.

Harwin S, Lucieer A. (2012) Assessing the Accuracy of Georeferenced Point Clouds Produced via Multi-View Stereopsis from Unmanned Aerial Vehicle (UAV) Imagery. Remote Sensing; 4(6):1573-1599.

Li, Z., Zhu, C., & Gold, C. (2010). Digital terrain modeling: principles and methodology. CRC press.

Lejot, J., Delacourt, C., Piégay, H., Fournier, T., Trémélo, M. L., & Allemand, P. (2007). Very high spatial resolution imagery for channel bathymetry and topography from an unmanned mapping controlled platform. Earth Surf. Proc. Land., 32(11), 1705-1725.

Priestnall, G., Jaafar, J., & Duncan, A. (2000). Extracting urban features from LiDAR digital surface models. Computers, Env.Urb. Systems, 24(2), 65-78.

Van der Meer, F., Hecker, C., van Ruitenbeek, F., van der Werff, H., de Wijkerslooth, C., & Wechsler, C. (2014). Geologic remote sensing for geothermal exploration: A review. Int. J. App. Earth Obs. and Geoinformation, 33, 255-269.